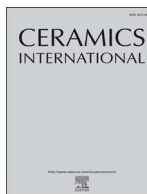




ELSEVIER

Contents lists available at ScienceDirect

Ceramics International

journal homepage: www.elsevier.com/locate/ceramint

Phase development and hydration kinetics of belite-calcium sulfoaluminate cements at different curing temperatures



Maruša Borštnar^{a,b,*}, Nina Daneu^c, Sabina Dolenc^a

^a Slovenian National Building and Civil Engineering Institute, Dimičeva ulica 12, 1000, Ljubljana, Slovenia

^b Jožef Stefan International Postgraduate School, Jamova cesta 39, 1000, Ljubljana, Slovenia

^c Jožef Stefan Institute, Jamova cesta 39, 1000, Ljubljana, Slovenia

ARTICLE INFO

Keywords:

Hydration
Cement
Temperature
Belite
Calcium sulfoaluminate

ABSTRACT

The influence of different curing temperatures on the hydration of belite-calcium sulfoaluminate cement was investigated at 20, 40 and 60 °C. The hydration kinetics and the hydrated phase assemblages were studied by isothermal calorimetry, X-ray powder diffraction, differential thermal analysis and thermogravimetric analysis, as well as field emission scanning electron microscopy. The compressive strength development of the cement pastes was also determined. Results showed that, at early ages, hydration was faster and early compressive strength was higher at elevated temperatures than at ambient temperature. On the other hand, at late ages in cement pastes cured at 60 °C, the amount of ettringite decreased, leading to lower compressive strength, indicating that the degree of hydration was lower at higher temperatures. Moreover, at elevated temperatures prismatic ettringite crystals became smaller due to faster hydration. Other hydration products present were aluminium hydroxide, which is formed together with ettringite from the hydration of calcium sulfoaluminate and gypsum, and C–S–H which precipitates as a main hydration product of belite. Belite hydrated in a lesser amount, especially at 60 °C, when the lowest amount of C–S–H was observed.

1. Introduction

Belite-calcium sulfoaluminate cements are a new generation of low energy and low-CO₂ cements, and are considered an alternative to conventional Portland cement, reducing CO₂ emissions by up to 30% as they require less limestone due to the substitution in part by calcium sulfate [1–4]. Furthermore, these cements demand a lower firing temperature in the kiln (typically around 1250 °C) and thus also emit a lower amount of NO_x [4]. In addition, belite-calcium sulfoaluminate cement clinkers are more easily ground in comparison to Portland cement clinker due to their higher porosity [3–5]. The main phases present in BCSA cements are belite (Ca₂SiO₄ or C₂S in cement notation), calcium sulfoaluminate (Ca₄(AlO₂)₆SO₃ or C₄A₃S̄) and ferrite (Ca₂(Al,Fe)₂O₅ or C₄AF), followed by calcium sulfate (CaSO₄ or C̄S) [6] in a form of anhydride, gypsum or bassanite [7–11]. The amount of calcium sulfate controls the setting of calcium sulfoaluminate in cement paste and can modify the kinetics of the hydration process [7,8]. Depending on the amount and source of the raw materials or sintering conditions belite-calcium sulfoaluminate cements can also contain other minor phases such as gehlenite (Ca₂Al₂SiO₇ or C₂AS), mayenite (12CaO·7Al₂O₃ or C₁₂A₇), perovskite (CaTiO₃ or CT), periclase (MgO or

M), arcanite (K₂SO₄ or K̄S̄), magnetite (Fe₃O₄ or fF) and excess of lime (CaO or C) [12–15].

The hydration of belite-calcium sulfoaluminate cements is a complex process mainly due to the different minor phases in addition to main phases [12–14]. The hydration of calcium sulfoaluminate leads to the formation of ettringite (Ca₆Al₂(SO₄)₃(OH)₁₂·26H₂O or C₆S̄₃H₃₂) and aluminium hydroxide (Al(OH)₃ or AH₃), which contribute to the early strength of the cement [1,10]. When the source of sulfate is consumed, calcium monosulfate is formed (Ca₄Al₂(OH)₁₂·SO₄·6H₂O or C₄A₃S̄H₁₂) [1,5,10]. Furthermore, the hydration of the belite leads to the formation of calcium silicate hydrates (3CaO·SiO₂·4H₂O or C–S–H) and portlandite (Ca(OH)₂ or CH), which contributes to the late age strength of the cement [12,15,16]. Also, other phases such as strätlingite (Ca₂Al₂SiO₇·8H₂O or C₂ASH₈) and katoite (Ca₃Al₂(OH)₁₂ or C₃AH₆) can precipitate [16–18].

One of the main parameters influencing the hydration of cements is temperature. As a result of different environmental conditions and also heat which is produced during the hydration, cement materials are exposed and affected by different temperatures [19,20]. While studies mainly deal with the hydration of ordinary Portland cement, blended cements and calcium sulfoaluminate cements, the studies on the

* Corresponding author. Slovenian National Building and Civil Engineering Institute, Dimičeva ulica 12, 1000, Ljubljana, Slovenia.

E-mail address: marusa.borstnar@zag.si (M. Borštnar).

<https://doi.org/10.1016/j.ceramint.2020.05.029>

Received 9 February 2020; Received in revised form 6 April 2020; Accepted 2 May 2020

Available online 05 May 2020

0272-8842/ © 2020 The Authors. Published by Elsevier Ltd. This is an open access article under the CC BY license

(<http://creativecommons.org/licenses/by/4.0/>).

Table 1
Chemical composition of raw materials (in wt. %).

	Limestone	Flysch	Bottom ash	Calcined bauxite	Titanogypsum	Mill scale
SiO ₂	4.76	32.02	59.75	5.88	0.13	0.64
Al ₂ O ₃	0.86	7.74	18.73	87.69	1.16	0.34
Fe ₂ O ₃	0.51	3.49	10.03	1.89	0.04	97.96
CaO	51.51	28.83	5.63	0.06	32.62	0.82
MgO	0.90	1.69	2.20	0.52	0.04	0.29
SO ₃	0.09	0.07	0.15	0.17	45.39	0.09
Na ₂ O	0.61	0.54	1.01	0.08	0.06	0.67
K ₂ O	0.14	1.23	1.60	0.39	0.01	0.02
TiO ₂	0.04	0.38	0.53	3.71	0.62	0.01
LOI 950 °C	41.41	24.65	1.20	0.15	21.35	0.00

kinetics of hydration processes and formation of hydration products of belite-calcium sulfoaluminate cement cured at different temperatures are rare.

Studies on ordinary Portland cement and blended cements at increased temperatures showed that an increase of curing temperature leads to an increase of the hydration rate and consequently to an increased early strength development [19–25]. However, at elevated temperatures the compressive strength decrease at a later period of hydration, and furthermore it is lower at high temperatures in comparison to cement pastes hydrated at lower temperatures [20,21,24,26–28]. At elevated temperatures there is only a short time for the diffusion of dissolved ions and for hydration products to precipitate rapidly, resulting in a heterogeneous distribution of hydration products and increased coarse porosity, and therefore a decreased compressive strength [19–21,23–27,29,30]. At elevated temperatures C–S–H density is increased [27] and its polymerization is increased [21,31,32]. Lothenbach et al. [25] observed a decrease in the amount of ettringite and shorter ettringite needles at higher temperatures. On the other hand, at a later age at lower temperatures the hydration rate is decreased, compressive strength is increased and coarse porosity decreased [24–26,29,30] due to the longer diffusion of dissolved ions and the slower precipitation of hydration products, which lead to a more homogenous distribution of hydration products [25,26,29]. At lower temperatures C–S–H has a higher gel porosity and is less polymerized [32].

Recent studies that deal with the hydration of calcium sulfoaluminate cement at elevated temperatures revealed that at temperatures around 90 °C ettringite is unstable, loses water and decomposes to metaettringite, which can influence the mechanical properties of the cement paste [33,34]. With the further addition of water to metaettringite, ettringite forms again. Metaettringite decomposes to monosulfate under steaming conditions and causes the delayed formation of ettringite [33,34]. Jeong et al. [33] indicated that the compressive strength of samples cured at 90 °C was at 1 day of hydration lower than at 30 and 60 °C due to the decomposition of ettringite. Another study on calcium sulfoaluminate cement [11], where hydration was studied in the first 24 h, showed that at higher temperatures the hydration of calcium sulfoaluminate and gypsum was faster, resulting in the rapid formation of ettringite and a higher hydration rate. Also, there was no precipitation of katoite, which would probably cause a regression of compressive strength. Furthermore, increasing the temperature also results in fewer but larger pores [11].

As concerns the effect of temperature on the belite-calcium sulfoaluminate cements, until now only the heat of hydration at different temperatures (5, 23 and 38 °C) was studied with isothermal calorimetry

[12]. The results were similar to those on ordinary Portland cement and blended Portland cements, indicating that with increasing the temperature to 38 °C, strength development is more rapid than at ambient temperature. At lower temperatures (5 °C) the hydration reaction is significantly slower [12].

The aim of this study was to investigate the effects of different curing temperatures on the hydration of belite – calcium sulfoaluminate cement. The composition of hydration products and microstructure at 1, 7, 28 and 90 days of hydration was studied using differential thermal analysis and thermogravimetric analysis, X-ray powder diffraction and Rietveld refinement, as well as field emission scanning electron microscopy. Furthermore, hydration kinetics was studied with isothermal calorimetry and the compressive strength development of the cement pastes was determined.

2. Experimental

2.1. Materials

The cement clinker with the targeted phase composition 65 wt% belite (C₂S), 20 wt% calcium sulfoaluminate (C₄A₃S̄) and 10 wt% ferrite (C₄AF) was synthesized for the study [35]. The clinkers were prepared of the following raw materials: limestone, flysch (sequence of sedimentary rock layers of calcareous breccia, calcareous sandstones and marls), bottom ash from a coal thermal power plant, white titanogypsum, calcined bauxite and mill scale. Chemical composition of raw materials is given in (Table 1). The materials were proportioned by a modified Bogue method [12] (Table 2).

All the raw materials were ground to pass a 200 µm mesh sieve before making batch compositions. After homogenization, 200 g of raw meal was ground for 3 h in 200 mL of isopropanol using a ball mill (CAPCO Test Equipment Ball Mill Model 9VS) and then dried at 40 °C for 24 h. Pressed pellets of 15 g of the raw meal with the diameter 30 mm and height 13 mm were prepared using a HPM 25/5 press at 10.6 kN and subjected to heating to 1250 °C with a heating rate of 10 °C/min in a Protherm furnace PLF 160/9. The holding time at the final temperature was 60 min. Finally, cooling was natural in a closed furnace. The heating and cooling were carried out under oxidizing conditions.

The synthesized clinker was ground below 0.125 mm in a vibratory disc mill (SIEBTECHNIK Labor Scheibenschwingmühle TS. 250) and blended with 20.3 wt % of white titanogypsum. The amount of gypsum needed was calculated according to Chen & Juenger [12]. The cement made was ground to a Blaine fineness of 497 m²/kg using a ball mill (CAPCO Test Equipment Ball Mill Model 9VS).

Table 2
Amount of raw materials used in a raw meal (in wt. %).

	Limestone	Flysch	Bottom ash	Calcined bauxite	Titanogypsum	Mill scale
Amount (wt. %)	57.9	23.6	9.0	5.3	4.0	0.2

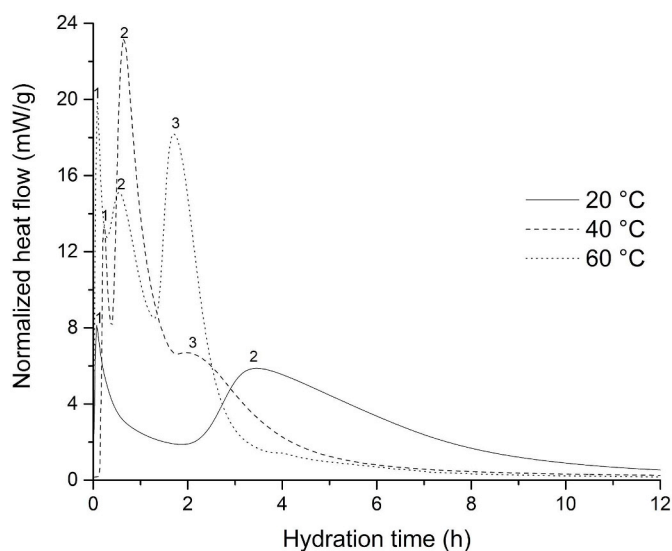


Fig. 1. Hydration heat flow for cement samples cured at 20, 40 and 60 °C.

Cement pastes were prepared using a water to cement/ratio of 0.4. Specimens were mixed by hand for 3 min and cast into prismatic moulds, 10 × 10 × 25 mm in size, demoulded after 24 h and cured in sealed plastic containers at 20, 40 and 60 °C until testing.

The hydration of the cement pastes was stopped by solvent exchange with isopropanol at 1, 7, 28 and 90 days. A part of the crushed cement paste from the interior (pieces close to the upper surface were discarded) was submerged in 100 mL of isopropanol for 15 min, filtered with a Buchner filter and rinsed twice with isopropanol. Samples were dried in a ventilated oven at 40 °C for 8 min [36].

2.2. Methods

The hydration kinetics of the cement was assessed by isothermal conduction calorimetry using an eight-channel TAM Air 8 calorimeter (TA Instruments). 4 g of the cement with a water/cement ratio of 0.4 was mixed in situ with an admix ampoule for 3 min. The heat evolution was evaluated for 7 days at 20, 40 and 60 °C on two replicate measurements per sample at a particular temperature.

The compressive strength of the cement pastes was measured on the prepared 10 × 10 × 25 mm prisms, cured at 20, 40 and 60 °C. The samples were demoulded after 24 h. The compressive strength was determined on four replicas per curing temperature at 1, 7, 28 and 90 days using ToniNORM, Toni Technic by Zwick testing machine with a loading rate of 0.05 kN/s.

X-ray powder diffraction was performed to determine the phase composition of the cement pastes with the hydration stopped at 1, 7, 28 and 90 days using a PANalytical Empyrean X-ray diffractometer equipped with CuK α radiation with $\lambda = 1.54 \text{ \AA}$. 5 g of the samples were ground in an agate mortar to a particle size below 0.063 mm. The ground powder was manually back-loaded into a circular sample holder (diameter 16 mm) to mitigate the preferred orientation effect for X-ray diffraction data collection. The samples were scanned at 45 kV and a current of 40 mA, over the 2θ range from 4° to 70°, at a scan rate of 0.026° 2θ /min and step time 172 s. The obtained X-ray diffraction patterns were analysed using X'Pert High Score Plus diffraction software v. 4.8 from PANalytical, using PAN ICSD v. 3.4 powder diffraction files. All Rietveld refinements were performed using the PANalytical X'Pert High Score Plus diffraction software, using the structures for the phases from ICDD PDF 4 + 2016 RDB powder diffraction files and publication references. The powder diffraction file (PDF) codes for the identified phases used for Rietveld refinements were: β -C₂S (01-086-0398), γ -C₂S (01-086-0391), C₄A₃S-orthorhombic (04-011-1786), C₄A₃S-cubic

(04-009-7268), C₄AF (01-071-0667) and C \bar{S} H₂ (00-33-0311), and C₆S₃H₃₂ (00-041-1451). The amorphous phase was not considered.

Thermogravimetric (DTA/TG) measurements of the cement pastes with stopped hydration at 1, 7, 28 and 90 days of hydration were carried out using a Netzsch STA 409 instrument in the temperature range from 30 to 1000 °C, at a heating rate of 10 °C/min, under nitrogen flow at a rate of 20 mL/min. The samples were ground to a particle size below 0.063 mm with an initial mass of approx. 15 mg and placed in Al₂O₃ crucibles. Measurements were performed on two replicas per curing temperature at 1, 7, 28 and 90 days. Results were analysed using the Netzsch Proteus Thermal Analysis software.

Freshly fractured surfaces of cement pastes with hydration stopped at 1, 7, 28 and 90 days were examined using a Field Emission Scanning Electron Microscope (FE/SEM) JEOL JSM-7600F equipped with an Energy Dispersive X-ray spectrometer (EDXS). All FE/SEM images were recorded at an accelerating voltage of 5 kV, a working distance of 15 mm and probe current 0.7 nA using backscattered electrons (BSE). Specimens were coated with a thin layer of platinum using Precision Etching Coating System (PECS Model682, Gatan, USA) to enhance electrical conductivity.

3. Results and discussion

3.1. Isothermal calorimetry

The results of the isothermal calorimetry are shown in Fig. 1. The first initial exothermic peak (labelled 1) was within the first 10–15 min for all samples, and is related to the wetting of the system and rapid dissolution of cement clinker phases, and an initial formation of hydration products [9–11,37,38]. The difference between the samples with different curing temperatures was evident, thus, the heat released during the initial period increased at elevated temperature.

The induction period following the initial peak was at ambient temperature with respect to the samples cured at a higher temperature much longer. Namely, while the induction period for the sample at 20 °C lasted for 3 h, for samples cured at an elevated temperature (40, 60 °C) is shortened to about 10 min. During the induction period, the clinker phases and gypsum slowly dissolve and ettringite slowly precipitates [9,37,38].

The acceleration period, when another exothermic (2) peak occurs, was exhibited around the 3rd hour of the hydration time for the samples cured at ambient temperature (20 °C), which however was shifted to an earlier time as the temperature was elevated. Accelerated hydration at elevated temperatures and therefore a faster dissolution of the anhydrous phases and precipitation of the hydrated phases was observed in Portland cement [23] and blended cements [11,23,39]. The acceleration period for the samples cured at 40 °C and 60 °C occurred after 75 min and 30 min, respectively. The acceleration peak could be attributed to the hydration reaction of calcium sulfoaluminate with gypsum and the formation of ettringite, as well as aluminium hydroxide [10,11].

Furthermore, as can be seen from the results, samples cured at 40 °C and 60 °C displayed another exothermic peak (labelled 3), which can be assigned to the further dissolution of gypsum and calcium sulfoaluminate, and the formation of ettringite and aluminium hydroxide [10]. However, at 40 °C, this peak was significantly smaller and rather represents a shoulder in comparison to 60 °C. Moreover, the difference was also observed in time periods as the corresponding times to these events were 2 h 15 min for a sample cured at 40 °C and 1 h 45 min for a sample cured at 60 °C.

The hydration rate slowed down earlier at elevated temperatures, after 5 h for samples cured at 40 and 60 °C, while for a sample cured at 20 °C after 12 h, meaning the initial reaction was faster at higher temperatures.

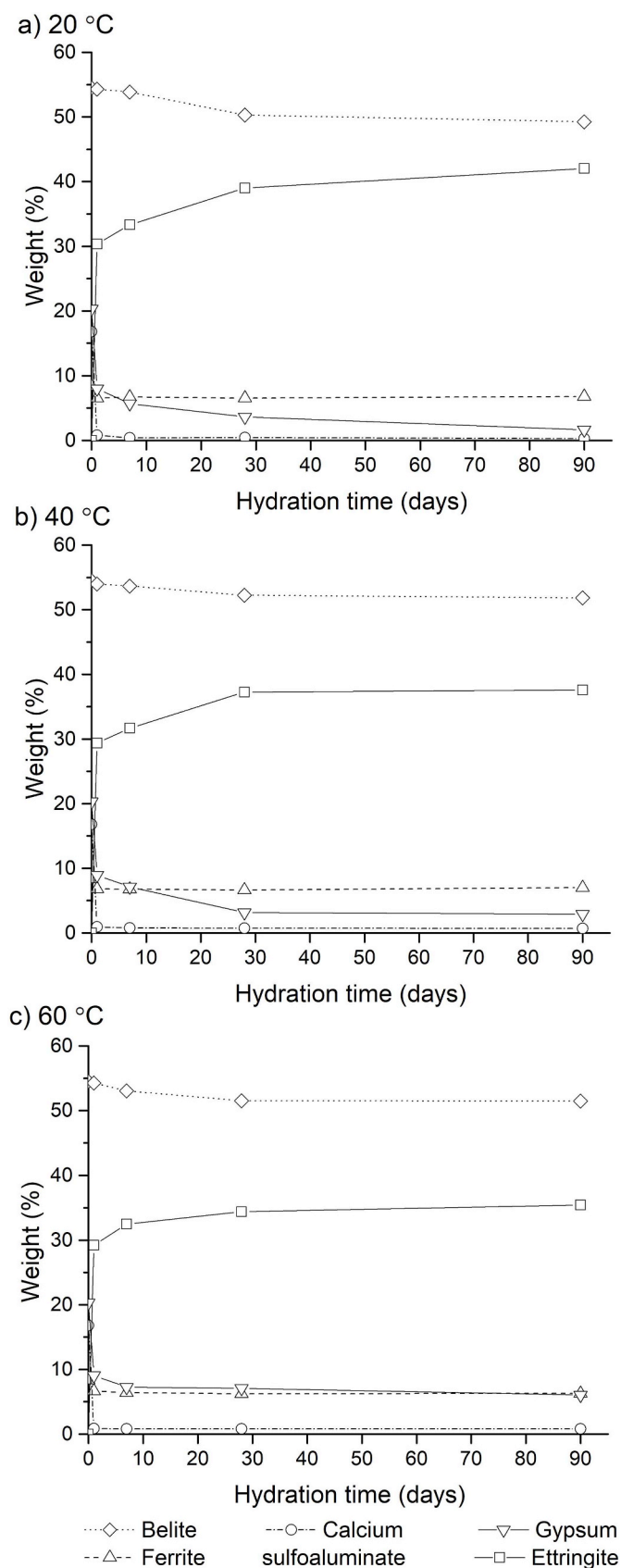


Fig. 2. Amounts of anhydrous phases and hydration products remained at different hydration times by Rietveld analysis at 20 °C, 40 °C and 60 °C.

3.2. X-ray powder diffraction

Fig. 2 shows the time-dependent evolution of the phases in the samples cured at different temperatures as calculated from the X-ray powder diffraction patterns using the Rietveld refinement. X-ray powder diffraction patterns of cement pastes cured at 20, 40 and 60 °C at 1, 7, 28 and 90 days of hydration are shown in Fig. 3.

The crystalline phases present in the cement pastes were belite, ferrite, calcium sulfoaluminate and gypsum as unhydrated relicts of the cement, while ettringite formed as a hydration product. Fig. 2 shows that the amount of calcium sulfoaluminate and belite clinker phases, as well as gypsum, decreased with time at all curing temperatures indicating the formation of hydration products. On the other hand, there was no notable difference in the amount of the ferrite phase with time or elevated temperature as ferrite reacts slower and is a less reactive phase in comparison to other clinker phases [40,41]. Most of the calcium sulfoaluminate has already reacted in the first 24 h of hydration with only less than 1 wt % remaining in the samples (Fig. 2a). Moreover, a significantly higher amount of non-reacted gypsum at 28 and 90 days of hydration was observed for the cement cured at 60 °C, which could be due to a lower degree of hydration at elevated temperatures (Fig. 2b and c). The amount of gypsum decreased continuously up to 28 days of hydration, after 28 days its amount was almost constant. Surplus gypsum was present in the cement pastes at all temperatures due to the high molar ratio of calcium sulfate to calcium sulfoaluminate beyond 4 [42]. Belite reacted only in lower amounts even at 90 days of hydration due to the high consumption of water by calcium sulfoaluminate and the consequently insufficient amount for belite to hydrate [43].

The hydrated phase identified in the samples, at ambient and elevated temperatures, was ettringite. The results indicated that the amount of ettringite increased with time as more hydrates precipitate from the hydration of the anhydrous phases. During the 28 days of hydration the amount of ettringite increased significantly at all temperatures. However, it is evident that at 40 and 60 °C the increase of the amount of ettringite after 28 days of hydration was almost negligible in comparison to 20 °C when the amount of ettringite still increased, suggesting a higher degree of hydration. Moreover, the amount of ettringite at 28 and 90 days of hydration was noticeably lower at 60 °C (Fig. 2c) than at 20 °C and 40 °C.

3.3. Differential thermal analysis/Thermogravimetric analysis

The results of the differential thermal analysis plotted in Fig. 4 are in agreement with the X-ray powder diffraction results, but also revealed the presence of some additional phases. The data indicated the presence of ettringite, C-S-H, aluminium hydroxide and gypsum.

The first and largest endothermic peak around 120 °C was attributed to ettringite and C-S-H [9,16,44]. Ettringite is formed with the hydration of calcium sulfoaluminate with calcium sulfate source [1,10], whereas C-S-H is formed with the hydration of belite [12,15,16]. As these two peaks overlap it is difficult to quantify the amount of the ettringite and C-S-H present in the samples. However, an increasing weight loss in this area with time (from 11.7% at 1 day to 15.8% at 90 days, 11.6%–14.2% and 12.6%–14.1% for 20, 40 and 60 °C, respectively) was observed, indicating the rising amount of ettringite and C-S-H.

A peak at 150 °C corresponds to the decomposition of gypsum. The differential thermal analysis and thermogravimetric analysis indicated that the amount of gypsum slightly decreased after 1–90 days (from the average 1.4% at 1 day to 1.1% at 90 days), since it is consumed in the hydration process (Fig. 4a and b).

An endothermic peak at 250 °C could be assigned to aluminium hydroxide [9,16,44], which was not detectable with X-ray powder diffraction due to its amorphous character [42,45]. The amount of aluminium hydroxide, that precipitates from the reaction of calcium

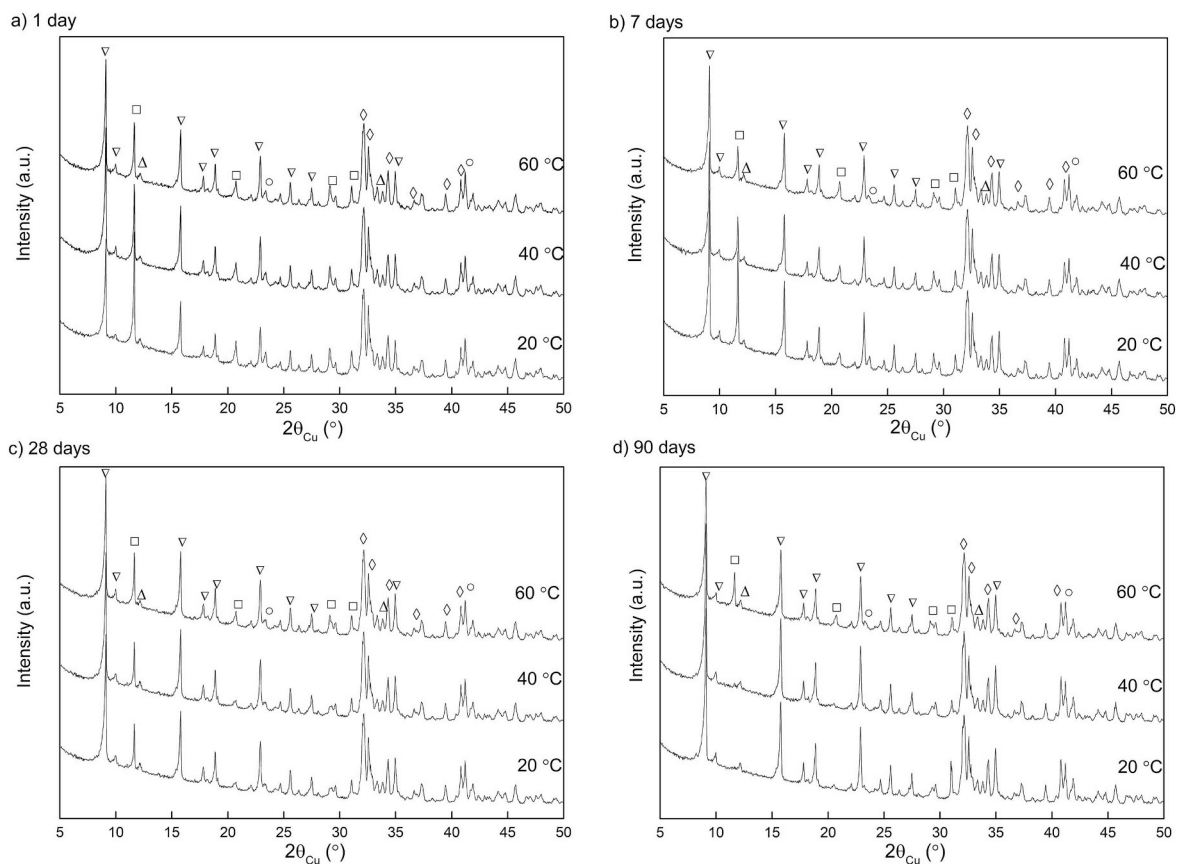


Fig. 3. X-ray powder diffraction patterns of cement pastes cured at 20, 40 and 60 °C. ∇ – ettringite, □ – gypsum, ○ – calcium sulfoaluminate, ◇ – belite, Δ – ferrite.

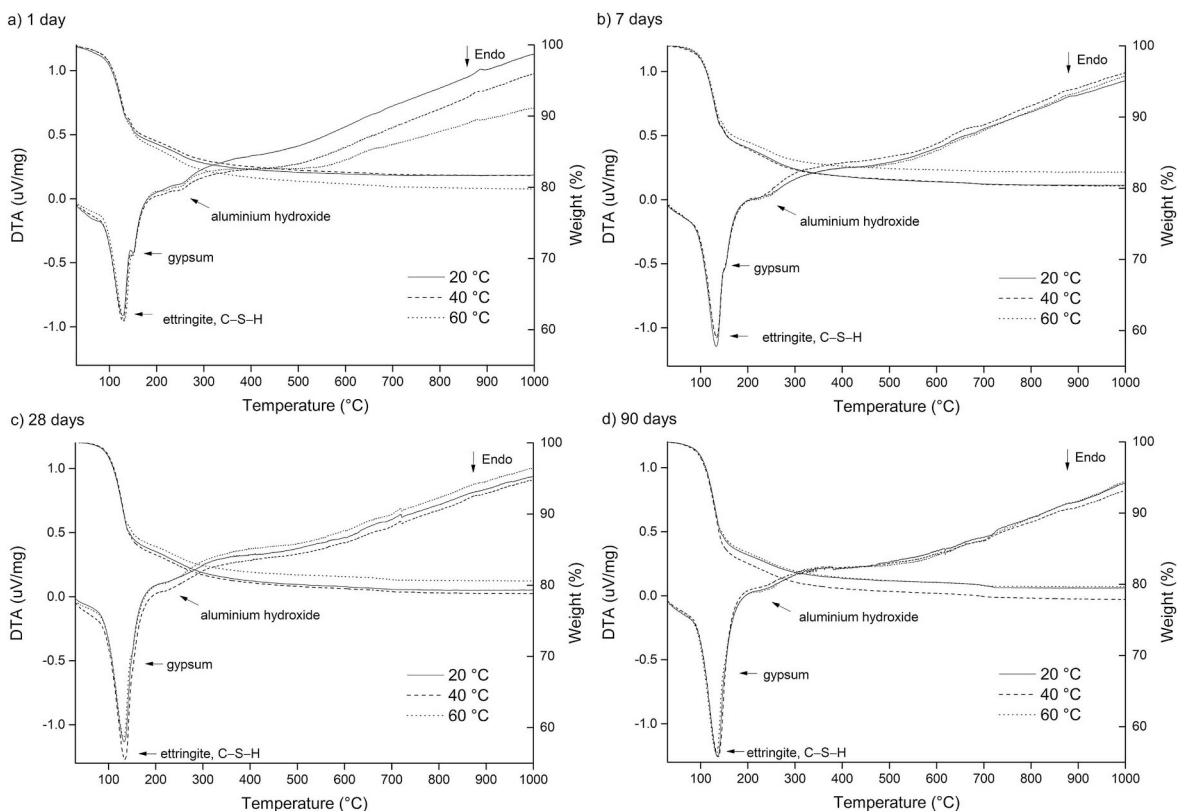


Fig. 4. Results of differential thermal and thermogravimetric analysis of cement pastes at different curing temperatures.

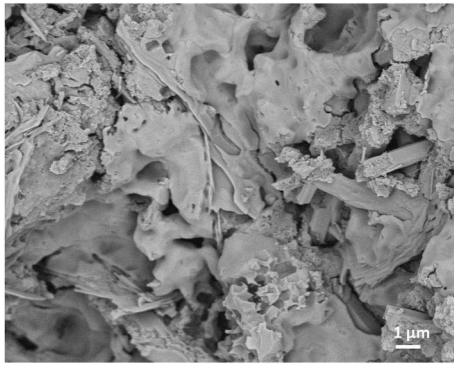


Fig. 5. FE/SEM microphotographs of cement paste at ambient temperature at 1 day of hydration where due to slow hydration at early age anhydrous gel-like clinker is observed.

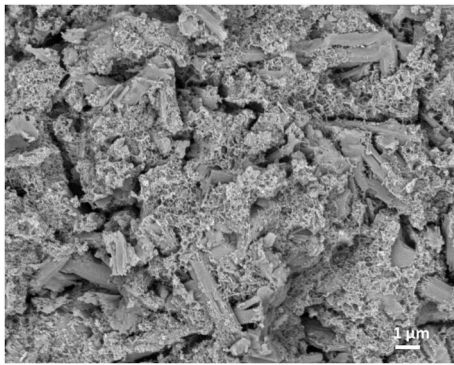


Fig. 6. FE/SEM microphotographs of cement paste cured at 40 °C at 28 days of hydration. Lower amount of clinker is present due to the formation of ettringite and C-S-H.

sulfoaluminate with gypsum and water, together with ettringite [1,10], did not change significantly with time or elevated temperatures (Fig. 4c and d).

3.4. Field emission scanning electron microscopy

The influence of temperature on the development of the microstructure and the development of different phases was furthermore studied using a field emission scanning electron microscope. The analyses revealed the presence of clinker relicts and non-reacted gypsum in addition to the hydration products ettringite and C-S-H.

In general, the amount of clinker relicts decreased with time at all curing temperatures, due to the formation of hydration products, which is in accordance with the X-ray powder diffraction and thermal

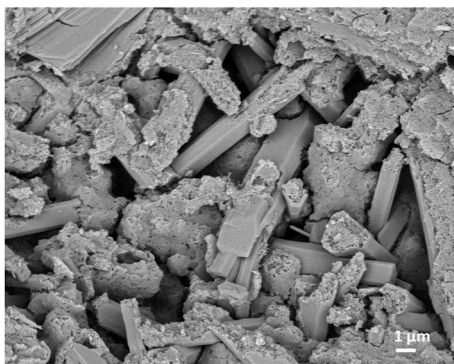


Fig. 7. FE/SEM microphotographs of cement paste showing long prismatic ettringite crystals in samples cured at 20 °C temperature at 7 days of hydration.

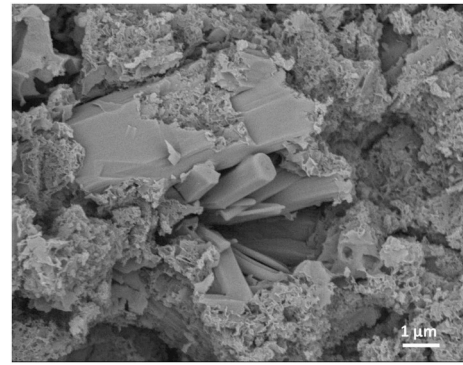


Fig. 8. FE/SEM microphotographs of cement paste cured at 60 °C at 7 days of hydration with smaller and less abundant ettringite crystals.

analysis. At 1-day of hydration in the samples cured at 20 °C gel-like clinker grains (Fig. 5) were observed, due to the slower hydration at an early age with respect to higher temperatures where anhydrous gel-like clinker was not observed due to accelerated hydration. Over 28 days the amount of clinker decreased slowly, whereas at 28 and 90 days of hydration its amount was significantly lower at all curing temperatures (Fig. 6). Similarly, the amount of gypsum decreased with time as well as the amount of clinker.

Ettringite as one of the hydration products was present in all the samples, but its amount at 28 days of hydration was the most prominent at 20 and 40 °C in comparison to 60 °C when its amount was the lowest. The amount of ettringite increased with time as the hydration continued. Up to 28 days of hydration the amount of newly precipitated ettringite increased quickly at all curing temperatures, while at 28 and 90 days the amount of ettringite did not change significantly, which support the X-ray diffraction results. The length of ettringite crystals in the samples at 20 °C after 1 day of hydration was on average up to 7 μm and 2 μm wide (Fig. 7) and it increased with time. With higher temperatures the size of the ettringite continued to become smaller, thus at 60 °C is on average 3 μm long and 1 μm wide (Fig. 8). These observations were also indicated by Lothenbach et al. [25], due to the faster formation of ettringite at elevated temperatures. Furthermore, the results showed that the size of the ettringite was the smallest at 1 day of hydration and increased with time. Ettringite crystals are prismatic with a hexagonal cross-section (Fig. 8) that became better developed with time.

In addition, by using the field emission scanning electron microscopy C-S-H was identified. This phase precipitated from the hydration of the belite phase and mainly covered the surface of the clinker relicts and gypsum, whereas ettringite crystals were covered to a lesser extent (Figs. 7 and 8). The amount of C-S-H increased with time. However, at 1 and 7 days of hydration a lower amount of C-S-H was present,

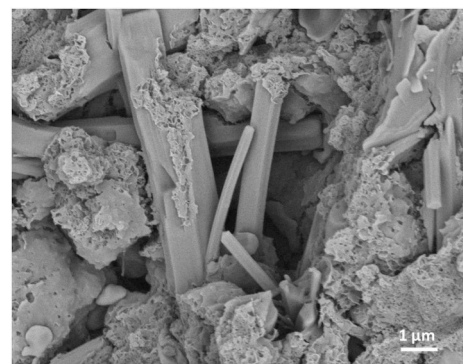


Fig. 9. FE/SEM microphotographs of flake-like C-S-H in cement paste cured at 20 °C at 1 day of hydration.

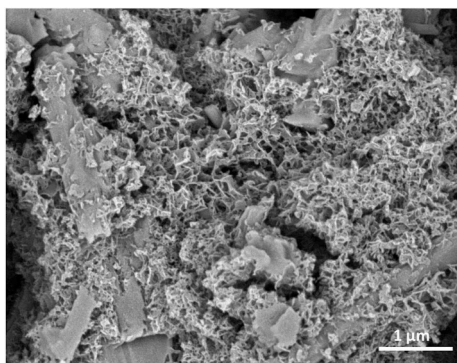


Fig. 10. FE/SEM microphotographs of honeycomb-like C–S–H in cement paste cured at 60 °C at 28 day of hydration.

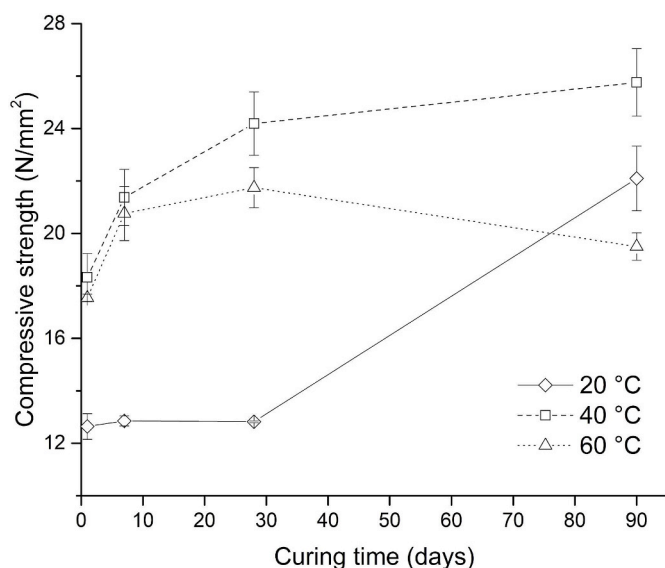


Fig. 11. Compressive strength development of cement pastes cured at different temperatures.

whereas after 28 days it increased significantly and continuously up to 90 days of hydration at all curing temperatures. Its amount decreased with elevated temperatures, especially at 60 °C after 28 and 90 days of hydration. These observations are also in agreement with the previous literature data, which indicated that due to accelerated hydration at higher temperatures hydration dissolved ions do not have enough time to dissolve before the formation of new hydration products, which lead to denser and more polymerized C–S–H and higher porosity, and therefore a decrease in compressive strength [19,20,25]. The results are in accordance with the X-ray powder diffraction, therefore the amount of unhydrated belite is higher in the samples cured at elevated temperatures, where the amount of C–S–H, which precipitated with the hydration of belite, is lower. The results showed that C–S–H is flake-like (Fig. 9) but became more honeycomb-like (Fig. 10) at higher temperatures and later ages. This is the most evident in samples cured at 60 °C after 28 and 90 days of hydration, where it can also be observed that the fibres became longer and thicker as observed by Zhang et al. [46].

3.5. Compressive strength

The effect of different temperatures on the compressive strength evolution of the cement pastes can be seen in Fig. 11.

At the early ages of the hydration, the compressive strength gain was significantly lower at 20 °C with respect to elevated temperatures.

For instance, the 1-day compressive strength of the sample cured at 20 °C was much lower (1.6 N/mm²) with respect to the other two samples where no evident difference was observed (18.3 N/mm² and 17.5 N/mm² for samples cured at 40 °C and 60 °C, respectively). The results showed that temperature mainly affected early age strength development, while at the 90 days of hydration the compressive strength values for samples cured at 20 °C were close to the samples cured at elevated temperature. These findings were also reported in other studies [19,20,23], where due to accelerated hydration reactions compressive strength increased with higher curing temperature. These results are also in accordance with the results obtained by isothermal calorimetry, where it can be seen that hydration is accelerated at elevated temperatures. Furthermore at 1-day of hydration in the samples cured at 20 °C, an anhydrous gel-like clinker was observed, due to the slower hydration at an early age, which is confirmed with the compressive strength results. The results also support the X-ray powder diffraction data since the amount of ettringite increased with time as well as compressive strength.

As seen from Fig. 11, the compressive strength of cement cured at 20 °C did not change significantly until 28 days, when it increased sharply due to the hydration of the belite phase and the formation of C–S–H. After 7 days of hydration the two samples hydrated at 40 and 60 °C show similar compressive strength development. While compressive strength at 40 °C increased steadily with time, the strength evolution after 28 days for samples cured at 60 °C decreased. Namely, at 90 days of hydration, the compressive strength of cement cured at 60 °C was the lowest (19.5 N/mm²) in comparison to 20 and 40 °C (22.1 N/mm² and 25.2 N/mm² for samples cured at 20 °C and 40 °C, respectively). In accordance, while the lowest compressive strength at 90 days of hydration and also the lowest amount of ettringite was indicated for samples cured at 60 °C. According to previous studies this may be due to higher porosity due to denser C–S–H and heterogeneous distribution of hydration products in cement paste [19,21], or to the decomposition of ettringite to metaettringite [33].

4. Conclusions

The influence of temperature on the hydration kinetics, formation of phase assemblage, microstructure and compressive strength of belite-calcium sulfoaluminate cement was studied at 20, 40 and 60 °C.

At higher temperatures, cement reacted earlier and released more heat during hydration in comparison to ambient temperature. Also, the compressive strength results showed that early strength was significantly higher at elevated temperatures than at ambient temperature. Furthermore, at 90 days of hydration, the compressive strength at 60 °C decreased and was the lowest, which corresponds to the higher amount of non-reacted gypsum and lower amount of precipitated ettringite at 90 days of hydration and suggests that at a higher temperature the degree of hydration was lower. On the other hand, due to the faster hydration of calcium sulfoaluminate at elevated temperatures the size of the prismatic ettringite crystals was smaller at higher temperatures. Besides ettringite, aluminium hydroxide was also formed with the hydration of calcium sulfoaluminate and gypsum with water. The hydration of belite yielded C–S–H, which covered the surface of other phases. The amount of C–S–H decreased at higher temperatures due to a lower degree of reaction at elevated temperatures. Furthermore, the shape of C–S–H changed from flake-like to honeycomb-like with an increase in temperature and time.

Declaration of competing interest

The authors declare that they have no known competing financial interests or personal relationships that could have appeared to influence the work reported in this paper.

Acknowledgments

The research is performed within the Young researcher programme and is financially supported by the Slovenian Research Agency, contract number 1000-18-1502.

References

- [1] A.J.M. Cuberos, Á.G. De la Torre, G. Álvarez-Pinazo, M.C. Martín-Sedeño, K. Schollbach, H. Pöllmann, M.A.G. Aranda, Active iron-rich belite sulfoaluminate cements: clinkering and hydration, *Environ. Sci. Technol.* 44 (2010) 6855–6862, <https://doi.org/10.1021/es101785n>.
- [2] E. Gartner, T. Sui, Alternative cement clinkers, *Cement Concr. Res.* 114 (2018) 27–39, <https://doi.org/10.1016/j.cemconres.2017.02.002>.
- [3] E. Gartner, Industrially interesting approaches to “low-CO₂” cements, *Cement Concr. Res.* 34 (2004) 1489–1498, <https://doi.org/10.1016/j.cemconres.2004.01.021>.
- [4] K. Quillin, Performance of belite–sulfoaluminate cements, *Cement Concr. Res.* 31 (2001) 1341–1349, [https://doi.org/10.1016/S0008-8846\(01\)00543-9](https://doi.org/10.1016/S0008-8846(01)00543-9).
- [5] G.S. Li, G. Walenta, E. Gartner, Formation and hydration of low CO₂ cements based on belite, calcium sulfoaluminate and calcium aluminoferrite, *Proceedings of the 12th ICC, Canada, Montreal, 2007*, pp. 9–12.
- [6] F. Winnefeld, B. Lothenbach, Phase equilibria in the system Ca₄Al₆O₁₂SO₄ – Ca₂SiO₄ – CaSO₄ – H₂O referring to the hydration of calcium sulfoaluminate cements, *RILEM Tech. Lett.* 1 (2016) 10–16, <https://doi.org/10.21809/rilemtechlett.v1.5>.
- [7] M. García-Maté, A.G. De la Torre, L. León-Reina, E.R. Losilla, M.A.G. Aranda, I. Santacruz, Effect of calcium sulfate source on the hydration of calcium sulfoaluminate eco-cement, *Cement Concr. Compos.* 55 (2015) 53–61, <https://doi.org/10.1016/j.cemconcomp.2014.08.003>.
- [8] M.C.G. Juenger, F. Winnefeld, J.L. Provis, J.H. Ideker, Advances in alternative cementitious binders, *Cement Concr. Res.* 41 (2011) 1232–1243, <https://doi.org/10.1016/j.cemconres.2010.11.012>.
- [9] F. Winnefeld, S. Barlag, Calorimetric and thermogravimetric study on the influence of calcium sulfate on the hydration of ye’elimite, *J. Therm. Anal. Calorim.* 101 (2010) 949–957, <https://doi.org/10.1007/s10973-009-0582-6>.
- [10] F. Winnefeld, B. Lothenbach, Hydration of calcium sulfoaluminate cements — experimental findings and thermodynamic modelling, *Cement Concr. Res.* 40 (2010) 1239–1247, <https://doi.org/10.1016/j.cemconres.2009.08.014>.
- [11] L. Zhang, F.P. Glasser, Hydration of calcium sulfoaluminate cement at less than 24 h, *Adv. Cement Res.* 14 (2002) 15, <https://doi.org/10.1680/adcr.2002.14.4.141>.
- [12] I.A. Chen, M.C.G. Juenger, Synthesis and hydration of calcium sulfoaluminate-belite cements with varied phase compositions, *J. Mater. Sci.* 46 (2011) 2568–2577, <https://doi.org/10.1007/s10853-010-5109-9>.
- [13] F.P. Glasser, L. Zhang, High-performance cement matrices based on calcium sulfoaluminate–belite compositions, *Cement Concr. Res.* 31 (2001) 1881–1886, [https://doi.org/10.1016/S0008-8846\(01\)00649-4](https://doi.org/10.1016/S0008-8846(01)00649-4).
- [14] J. Majling, S. Sahu, M. Vlna, D.M. Roy, Relationship between raw mixture and mineralogical composition of sulfoaluminate belite clinkers in the system CaO–SiO₂–Al₂O₃–Fe₂O₃–SO₃, *Cement Concr. Res.* 23 (1993) 1351–1356, [https://doi.org/10.1016/0008-8846\(93\)90072-H](https://doi.org/10.1016/0008-8846(93)90072-H).
- [15] F. Bullerjahn, D. Schmitt, M. Ben Haha, Effect of raw mix design and of clinkering process on the formation and mineralogical composition of (ternesite) belite calcium sulfoaluminate ferrite clinker, *Cement Concr. Res.* 59 (2014) 87–95, <https://doi.org/10.1016/j.cemconres.2014.02.004>.
- [16] G. Álvarez-Pinazo, I. Santacruz, M.A.G. Aranda, Á.G. De la Torre, Hydration of belite–ye’elimite–ferrite cements with different calcium sulfate sources, *Adv. Cement Res.* 28 (2016) 529–543, <https://doi.org/10.1680/adcr.16.00030>.
- [17] B. Lothenbach, B. Albert, M. Vincent, G. Ellis, Hydration of Belite–Ye’elimite–Ferrite cements: thermodynamic modeling, *14th International Conference on the Chemistry of Cement, Beijing, China, 2015*, p. 12.
- [18] Y. Jeong, C.W. Hargis, S.-C. Chun, J. Moon, The effect of water and gypsum content on strätlingite formation in calcium sulfoaluminate-belite cement pastes, *Construct. Build. Mater.* 166 (2018) 712–722, <https://doi.org/10.1016/j.conbuildmat.2018.01.153>.
- [19] F. Deschner, B. Lothenbach, F. Winnefeld, J. Neubauer, Effect of temperature on the hydration of Portland cement blended with siliceous fly ash, *Cement Concr. Res.* 52 (2013) 169–181, <https://doi.org/10.1016/j.cemconres.2013.07.006>.
- [20] I. Elkhadiri, F. Puertas, The effect of curing temperature on sulphate-resistant cement hydration and strength, *Construct. Build. Mater.* 22 (2008) 1331–1341, <https://doi.org/10.1016/j.conbuildmat.2007.04.014>.
- [21] I. Elkhadiri, M. Palacios, F. Puertas, Effect of curing temperature on cement hydration, *Ceramics* 53 (2009) 65–75.
- [22] W. Ma, D. Sample, I.R. Martin, P.W. Brown, Calorimetric Study of Cement Blends Containing Fly Ash, Silica Fume, and Slag at Elevated Temperatures, (1994), p. 7.
- [23] J.I. Escalante-García, J.H. Sharp, The effect of temperature on the early hydration of Portland cement and blended cements, *Adv. Cement Res.* 12 (2000) 121–130, <https://doi.org/10.1680/adcr.2000.12.3.121>.
- [24] J.I. Escalante-García, J.H. Sharp, Effect of temperature on the hydration of the main clinker phases in portland cements: part I, neat cements, *Cement Concr. Res.* 28 (1998) 1245–1257, [https://doi.org/10.1016/S0008-8846\(98\)00115-X](https://doi.org/10.1016/S0008-8846(98)00115-X).
- [25] B. Lothenbach, F. Winnefeld, C. Alder, E. Wieland, P. Lunck, Effect of temperature on the pore solution, microstructure and hydration products of Portland cement pastes, *Cement Concr. Res.* 37 (2007) 483–491, <https://doi.org/10.1016/j.cemconres.2006.11.016>.
- [26] K.O. Kjellsen, R.J. Detwiler, O.E. Gjorv, Development of microstructures in plain cement pastes hydrated at different temperatures, *Cement Concr. Res.* 21 (1991) 179–189, [https://doi.org/10.1016/0008-8846\(91\)90044-1](https://doi.org/10.1016/0008-8846(91)90044-1).
- [27] B. Lothenbach, T. Matschei, G. Möschner, F.P. Glasser, Thermodynamic modelling of the effect of temperature on the hydration and porosity of Portland cement, *Cement Concr. Res.* 38 (2008) 1–18, <https://doi.org/10.1016/j.cemconres.2007.08.017>.
- [28] Y. Maltais, J. Marchand, Influence of curing temperature on cement hydration and mechanical strength development of fly ash mortars, *Cement Concr. Res.* 27 (1997) 1009–1020, [https://doi.org/10.1016/S0008-8846\(97\)00098-7](https://doi.org/10.1016/S0008-8846(97)00098-7).
- [29] K.O. Kjellsen, R.J. Detwiler, O.E. Gjorv, Backscattered electron imaging of cement pastes hydrated at different temperatures, *Cement Concr. Res.* 20 (1990) 308–311, [https://doi.org/10.1016/0008-8846\(90\)90085-C](https://doi.org/10.1016/0008-8846(90)90085-C).
- [30] K. De Weerd, M. Ben Haha, G. Le Saout, K.O. Kjellsen, H. Justnes, B. Lothenbach, The effect of temperature on the hydration of composite cements containing limestone powder and fly ash, *Mater. Struct.* 45 (2012) 1101–1114, <https://doi.org/10.1617/s11527-011-9819-5>.
- [31] T.T.H. Bach, C.C.D. Coumes, I. Pochard, C. Mercier, B. Revel, A. Nonat, Influence of temperature on the hydration products of low pH cements, *Cement Concr. Res.* 42 (2012) 805–817, <https://doi.org/10.1016/j.cemconres.2012.03.009>.
- [32] A. Bentur, R.L. Berger, J.H. Kung, N.B. Milestone, J.F. Young, Structural properties of calcium silicate pastes: II, effect of curing temperature, *J. Am. Ceram. Soc.* 62 (1979) 362–366, <https://doi.org/10.1111/j.1151-2916.1979.tb19079.x>.
- [33] Y. Jeong, C.W. Hargis, H. Kang, S.-C. Chun, J. Moon, The effect of elevated curing temperatures on high ye’elimite calcium sulfoaluminate cement mortars, *Materials* 12 (2019) 1072, <https://doi.org/10.3390/ma12071072>.
- [34] J. Kaufmann, F. Winnefeld, B. Lothenbach, Stability of ettringite in CSA cement at elevated temperatures, *Adv. Cement Res.* 28 (2016) 251–261, <https://doi.org/10.1680/adcr.15.00029>.
- [35] L. Žibret, A. Ipavec, S. Kramar, Microstructure of belite sulfoaluminate clinker and its influence on clinker reactivity, *International Workshop on Calcium Sulfoaluminate Cements, Murten, Switzerland, 2018*, p. 1.
- [36] R. Snellings, J. Chwast, Ö. Cizer, N. Belie, Y. Dhandapani, P. Durdziński, J. Elsen, J. Haufe, D. Hooton, C. Patapy, M. Santhanam, K. Scrivener, D. Snoeck, L. Steger, S. Tongbo, A. Vollpracht, F. Winnefeld, B. Lothenbach, RILEM TC-238 SCM Recommendation on Hydration Stoppage by Solvent Exchange for the Study of Hydrate Assemblages, *Materials and Structures*, (2018), p. 51, <https://doi.org/10.1617/s11527-018-1298-5>.
- [37] Y. Shen, X. Li, X. Chen, W. Zhang, D. Yang, Synthesis and calorimetric study of hydration behavior of sulfate-rich belite sulfoaluminate cements with different phase compositions, *J. Therm. Anal. Calorim.* 133 (2018) 1281–1289, <https://doi.org/10.1007/s10973-018-7251-6>.
- [38] A. Rungchetch, C.S. Poon, P. Chindaprasirt, K. Pimraksa, Synthesis of low-temperature calcium sulfoaluminate-belite cements from industrial wastes and their hydration: comparative studies between lignite fly ash and bottom ash, *Cement Concr. Compos.* 83 (2017) 10–19, <https://doi.org/10.1016/j.cemconcomp.2017.06.013>.
- [39] I.G. Richardson, C.R. Wilding, M.J. Dickson, The hydration of blastfurnace slag cements, *Adv. Cement Res.* 2 (1989) 147–157, <https://doi.org/10.1680/adcr.1989.2.8.147>.
- [40] W. Kurdowski, *Cement and Concrete Chemistry*, Springer, New York, 2014 Dordrecht.
- [41] N.B. Winter, *Understanding Cement: an Introduction to Cement Production, Cement Hydration and Deleterious Processes in Concrete*, Microanalysis Consultants, 2012.
- [42] F. Winnefeld, L.H.J. Martin, C.J. Müller, B. Lothenbach, Using gypsum to control hydration kinetics of CSA cements, *Construct. Build. Mater.* 155 (2017) 154–163, <https://doi.org/10.1016/j.conbuildmat.2017.07.217>.
- [43] H. Beltagui, G. Jen, M. Whittaker, M.S. Imbabi, The influence of variable gypsum and water content on the strength and hydration of a belite-calcium sulfoaluminate cement, *Adv. Appl. Ceram.* 116 (2017) 199–206, <https://doi.org/10.1080/17436753.2017.1289722>.
- [44] K. Scrivener, R. Snellings, B. Lothenbach (Eds.), *A Practical Guide to Microstructural Analysis of Cementitious Materials*, first ed., CRC Press, 2018, <https://doi.org/10.1201/b19074>.
- [45] M. Ben Haha, F. Winnefeld, A. Pisch, Advances in understanding ye’elimite-rich cements, *Cement Concr. Res.* 123 (2019) 105778, <https://doi.org/10.1016/j.cemconres.2019.105778>.
- [46] Z. Zhang, G.W. Scherer, A. Bauer, Morphology of cementitious material during early hydration, *Cement Concr. Res.* 107 (2018) 85–100, <https://doi.org/10.1016/j.cemconres.2018.02.004>.